Available online at www.sciencedirect.com
SCIENCE DIRECT®
Chemical Physics 325 (2006) 178–184
Chemical Physics
www.elsevier.com/locate/chemphys

Influence of substrate morphology on organic layer growth: PTCDA on Ag(1 1 1)

H. Marchetto [a], U. Groh [b], Th. Schmidt [b,*], R. Fink [b,c], H.-J. Freund [a], E. Umbach [b]

[a] *Fritz-Haber-Institut der Max-Planck-Gesellschaft, Faradayweg 4-6, D-14195 Berlin, Germany*
[b] *Experimentelle Physik II, Universität Würzburg, Am Hubland, D-97074 Würzburg, Germany*
[c] *Physikalische Chemie II, Universität Erlangen-Nürnberg, Egerlandstraße 3, D-91058 Erlangen, Germany*

Received 30 November 2005; accepted 13 January 2006
Available online 7 February 2006

Abstract

By UV-excited photoelectron emission microscopy (UV-PEEM) we investigated the microscopic growth behavior of organic thin films using 3,4,9,10-perylene-tetracarboxylicacid dianhydride (PTCDA) on a Ag(1 1 1) single crystal substrate as example. Direct, real time observation allows to correlate the initial growth modes and the related kinetic parameters with substrate properties like terrace width, step density, and step bunches from the submonolayer range up to 5 layers or more. Above room temperature PTCDA grows in a Stranski–Krastanov fashion: after completion of the first two stable layers three-dimensional islands are formed. The nucleation density strongly depends on the temperature and the substrate morphology thus affecting the properties of the organic film.

Keywords: Photoelectron emission microscopy; OMBE; Growth kinetics; Nucleation

1. Introduction

The electrical and optical properties of organic films strongly depend on their structural and morphological properties. Ideal epitaxial growth resulting in perfect, nearly defect-free films requires optimum conditions [1]. This is particularly difficult in the heteroepitaxy of very different materials like, e.g., organic–inorganic heterostructures [2,3]. The problem with the preparation of such systems lies in the nature of the involved substances. Whereas the structural periodicity in inorganic compounds is on the scale of few Ångström, the dimensions of organic unit cells are usually in the range of nanometers. In addition, the anisotropic shape and intermolecular interaction, the very different thermal expansion coefficients, and the (partly excited) internal degrees of freedom, e.g., the soft vibrational and phonon modes, of condensed molecules may result in different structural modifications (polymorphoism) in the condensed phase and in unexpected growth behavior. Thus, imperfections at the interface which may extend into the growing film are foreseeable.

In the rapidly growing field of molecular electronics these organic–inorganic hybrid systems play an extremely important role, for instance in organic field-effect transistors, light-emitting devices, transponders, and solar cells. Structural imperfections may very negatively affect the performance of such devices. This is for instance true for the charge carrier injection at the interface and for the carrier mobility within the film which is hindered by traps and scattering at grain boundaries and defects as well as by the hopping barriers between non-equivalent neighboring molecules. Moreover, the optical properties may suffer from imperfections causing non-radiative decay channels, traps, and scattering centers for exciton transport, and they may change by varying molecular orientation, geometric structure, and film morphology as a function of organic film preparation [4].

The structural imperfections within a thin film which affect its quality and properties arise from the dynamical

* Corresponding author. Fax: +493063922990.
E-mail address: thomas.schmidt@physik.uni-wuerzburg.de (Th. Schmidt).

0301-0104/$ - see front matter © 2006 Elsevier B.V. All rights reserved.
doi:10.1016/j.chemphys.2006.01.006

growth behavior and from the properties of the interface. It is of course known from many studies of inorganic materials that imperfections of the underlying substrate may deteriorate the growth and structural properties of the film. However, the details and the extent of the influence of the substrate surface quality on organic layer growth have not been systematically investigated so far, and very few experimental results are yet available. In this paper, we particularly address the influence of the substrate on the initial growth of an epitaxial organic film. Emphasis is placed on the influence of the morphological properties of the metal substrate, in particular the effect of steps and step bunches on the growth behavior. The variation of the substrate temperature during adsorption of the molecules is another important parameter which directly affects the mobility and hence the growth behavior of the molecules.

For our investigation we have chosen the well-known model system 3,4,9,10-perylene-tetracarboxylicacid dianhydride (PTCDA) on a crystalline Ag(1 1 1) substrate. Due to the small (<2%) lattice mismatch between the (1 0 2) plane of the β-modification of the PTCDA single crystal and the commensurate superstructure of the PTCDA monolayer on the Ag(1 1 1) substrate, PTCDA can grow in a quasi-epitaxial manner [5]. In order to directly correlate the film properties with microscopic properties of the substrate we use photoelectron emission microscopy (PEEM), which is ideally suited to monitor in situ the properties of the substrate and the organic film during deposition of the molecules as already shown for a different organic system, pentacene on SiO_2 [6]. Monitoring the involved processes directly and in real time allows to observe metastable intermediate states and to extract kinetic parameters of the film at every growth state and to correlate them to mesoscopic distortions of the substrate surface.

2. Experimental

The photoelectron emission microscope (PEEM) used for the experiments was an intermediate setup of the energy-filtered and aberration-corrected SMART spectromicroscope [7,8], installed at the soft X-ray synchrotron radiation source BESSY-II (Berlin, Germany). This instrument enables a comprehensive in situ surface and thin film characterization in *real-time* by microscopic imaging, diffraction, and spectroscopy of photo-emitted and/or reflected electrons [9].

In the present study a mercury short arc lamp (Hg-lamp) was used as photon source ($h\nu = 4.9$ eV) for photoelectron excitation. In the case of a metal surface the intensity of the PEEM image and the image contrast are determined by two parameters: (i) the local work function; and (ii) the density of states (DOS) near the Fermi level. Since the clean Ag(1 1 1) surface has a work function Φ of 4.8 eV it appears bright in PEEM images.

The deposition of the first monolayer of PTCDA changes the PEEM intensity by three contributions: (j) it increases the work function to 4.9 eV (which is hardly changed upon further PTCDA deposition [10]) thus reducing the substrate emission by cutting off some fraction, (jj) it further reduces the substrate emission by elastic and inelastic scattering of the emitted substrate electrons (attenuation), and (jjj) it opens a new emission channel right below the Fermi level which arises from the hybridization (and partial filling) of the lowest unoccupied molecular level (LUMO) of PTCDA with the s-states of Ag [10]. Apparently, (j) and (jj) are the dominating influences on the PEEM contrast, as the first layer leads to a considerable reduction of the emission. The (intensity increasing) effect of (jjj) is apparently small which is most likely due to a low photoemission cross section in this photon energy range.

For the second and higher layers only contribution (jj) is applicable as the work function remains unchanged for these layers (j), and there is no occupied molecular orbital near the Fermi edge (jjj). For the second and thicker PTCDA layers the highest occupied molecular orbital (HOMO) has a binding energy of 2 eV [10] and hence cannot lead to photoemission using photons of $h\nu = 4.9$ eV taking the 4.9 eV work function into account. Thus, as seen in Figs. 1 and 2, the contrast of the different layers above the first layer is exclusively due to attenuation effects: most photoelectrons are excited in the Ag substrate and have to surpass the organic layers; due to scattering effects their intensity is almost exponentially attenuated by these layers. This monotonic decrease of the substrate intensity enables the identification of the local thickness up to about 8 layers

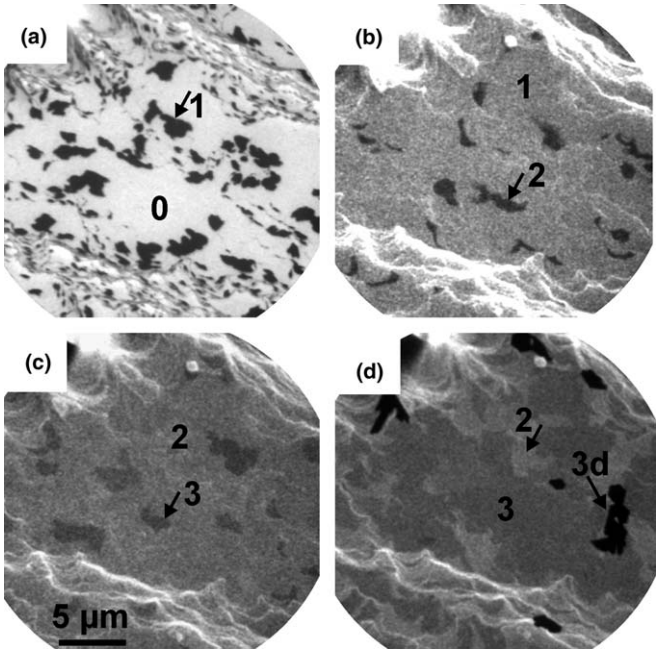

Fig. 1. In situ observation of the PTCDA growth on a Ag(1 1 1) surface at 378 K. The UV-PEEM images (a)–(d) show the identical area on the surface for the nominal coverages of 0.25, 1.05, 2.05, and 5 ML. The field of view is 23 μm × 23 μm. Only the intensity of image (a) was rescaled to optimize the contrast. The islands with the thickest PTCDA layer appear always darker than the surrounding. The labels 0, 1, 2, 3, and 3d indicate the pure substrate, the first to third layer, and the 3d-islands.

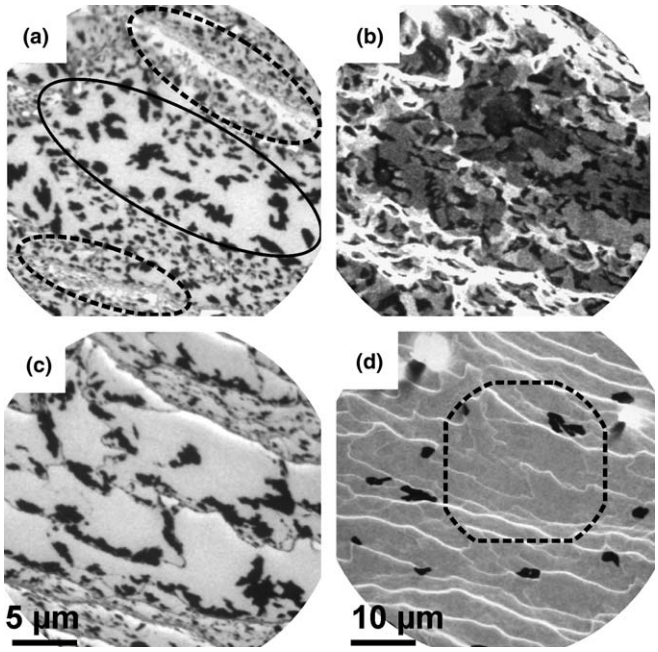

Fig. 2. PEEM images of the PTCDA growth on a Ag(1 1 1) surface at different substrate temperatures: images (a,b): $T = 320$ K, images (c,d): $T = 403$ K. For each temperature two images from a sequence of 300 images were selected for a nominal coverage of 0.25 ML (a,c) and 5 ML (b,d), respectively. The field of view is 23 μm × 23 μm (a–c) and 46 μm × 46 μm (d), respectively. For the identification of the layers refer to Fig. 1. The ellipses in (a) mark high (dashed lines) and low (solid line) step density regions. The marked area in (d) corresponds to the entire area of (c).

which is a remarkable finding and very useful for studying layer growth.

For the in situ preparation of PTCDA films a Knudsen cell type evaporator was installed pointing towards the sample under a grazing incidence angle of 20°. The organic material was cleaned before deposition by cycles of in vacuum re-sublimation. The deposition rate was chosen as about 0.2 ML/min in all experiments. This rate was optimized for the recording speed available at the time of the experiments. One layer (1 ML) is defined as the deposited amount required to saturate the first PTCDA layer on the Ag(1 1 1) surface at about 330 K, for which temperature desorption can be neglected. The sample was heated from the back side by irradiation from a heated filament for $T < 650$ K or by electron bombardment for $T > 650$ K. The temperature was measured with a W/WRe 26–5% thermocouple with an absolute accuracy of about 10 K at 400 K and a relative accuracy of 1 K. During deposition the substrate temperature was kept constant within 1 K. The base pressure of the microscope was below 3×10^{-10} mbar.

The orientation of the Ag (1 1 1) single crystal surface deviated about 0.2° from the ideal orientation, corresponding to an average atomic step distance of about 70 nm. After mechanical and chemical polishing the sample was cleaned in vacuum by several cycles of Argon ion sputtering at 600 eV and subsequent annealing at 750 K (heating rate about 20 K/min). This resulted in a clean (checked by XPS) and rather smooth surface. After several adsorption and cleaning cycles, however, the initially nearly regularly stepped surface was changed and decayed in an alternating sequence of micrometer wide smooth areas with a low density of single atomic steps (as seen in subsequent LEEM experiments [11]) and of rough areas with high step density leading to step bunches (>5 step bunches/μm^2). It is emphasized that we carefully verified that neither the high electric field at the sample nor the intense UV illumination affected the sample or the organic overlayer, i.e., no radiation damage or field effect influenced our findings.

3. Results and interpretation

3.1. Real-time observation of organic film growth

The four PEEM images of Fig. 1 show the PTCDA growth on a Ag(1 1 1) surface at a substrate temperature of 378 K. These images were selected from a sequence of images recorded in *real-time* during deposition (acquisition time: 4 s per image with 2 s dead time corresponding to about 50 images per monolayer). The image contrast of the PTCDA layer is due to the above mentioned differences in electron emission intensity (due to work function change and attenuation). The selected surface area consists of a flat region in the center of the images and areas of high step density (step bunches) in their upper and lower part. At 0.25 ML coverage (Fig. 1a) the step bunches in the rough surface areas appear as dark lines. This contrast is due to the decoration of steps by PTCDA molecules during the very initial growth of the first layer (below 0.04 ML) which is often termed inhomogeneous nucleation. This finding is in agreement with that of a previous STM investigation [5] which also indicated that steps may be attractive to the nucleation of PTCDA islands on the clean Ag(1 1 1) surface while they appear to be repulsive on Ag(1 1 0). From the present data, we can derive that at least not all substrate steps act as nucleation centers, because of the temperature dependence discussed below, but we cannot exclude that some islands start to grow at steps. As soon as the surface is fully covered with PTCDA (Fig. 1b–d), the step bunches appear bright as for the clean Ag(1 1 1) surface, because the work function at the steps is smaller than on the terraces, apparently also with adsorbed monolayer.

As clearly seen in the recorded movie, the first two PTCDA layers grow in an ideal layer-by-layer fashion (which is only indirectly seen in the selected snapshots of Fig. 1). Fig. 1(a)–(c) show the nucleation of the first three layers for nominal coverages of 0.25, 1.05, and 2.05 ML. The topmost PTCDA layer appears always dark in the (rescaled) images. The nucleation of the second and the third layer starts only after the layer underneath is fully completed. For the third layer, however, there is a competition of layer growth and 3D island formation. Thus, before the third layer is completed 3D islands (black in

Fig. 1d) are formed (second and third layer appear light and dark grey, respectively). From our growth studies at different substrate temperatures, it is derived that this type of Stranski–Krastanov growth (2 stable layers, then 3D-island formation) always occurs for temperatures slightly above room temperature [12].

In the following, we focus on the nucleation site and nucleation density for the different layers. It is remarkable that the positions of the nucleation sites differ from image to image, indicating that the nucleation sites are not determined by spot-wise modifications of the surface morphology or by grains of contamination. Nevertheless, the substrate morphology does influence the nucleation. There is a difference of the nucleation densities in rough and flat areas of the substrate which is most obvious in the low coverage range (Fig. 1a). In the rough area, the average size of the two-dimensional (2D) islands is significantly smaller than that in the smooth area (center) but their density is significantly higher. Moreover, the large 2D islands are mainly formed at the rim of the smooth area close to step bunches. At higher coverages (Fig. 1b–d) the overall nucleation density decreases and the island size increases.

3.2. Temperature dependence

The substrate temperature is an important parameter for the control of the growth process. The influence is demonstrated in Fig. 2 for a low (320 K, Fig. 2a and b) and a high temperature (403 K, Fig. 2c and d). The figure compares the situation for the two extremes of Fig. 1, i.e., the nucleation of the first layer (0.25 ML) and the situation after formation of 3D islands (nominal 5 ML).

The overall nucleation densities for the first layer and for the 3D islands are higher at 320 K (Fig. 2a and b) than at 403 K (Fig. 2c and d) indicating diffusion limited formation of nuclei. The corresponding densities at 378 K (compare Fig. 1a and d) fit in between. Note, that at 403 K the 3D nucleation density is so low, that the field of view had to be enlarged for the 5 ML coverage (Fig. 2d). The 0.25 ML images show an influence of the surface morphology for both temperatures. In Fig. 2a the smooth and rough areas are highlighted by solid and dashed lines, respectively. In the smooth area the 2D islands are considerably larger than in the rough areas, their density, however, is lower confirming the observation at 378 K (Fig. 1).

At 403 K the 2D islands of the first layer prefer nucleation sites near step bunches (Fig. 2c). The same is true for the 3D islands at 403 K (Fig. 2d). At 320 K the density of 3D islands is higher, so that nucleation also occurs on the smooth area between the step bunches. Beside the 3D islands (black in Fig. 2b) are areas which are up to five layers thick, which can be derived from the different grey levels. At this temperature the growth mode transfers from Stranski–Krastanov to quasi Frank–van der Merwe growth [13–15].

3.3. Influence of the substrate morphology on the growth kinetics

The *real-time* observation of the PTCDA growth was repeated for different temperatures. At specific coverages (0.25, 1.05 and 5 ML) we analyzed the nucleation density for the first and second layers and for the 3D islands. In Fig. 3 the nucleation densities are plotted on a logarithmic scale versus $1/T$ (Arrhenius-plot) for these coverages. The open and solid symbols distinguish between rough and smooth substrate areas, respectively, as indicated in the inset of Fig. 3a. For the first and second layer the analysis was done in a field of view of $23 \times 23\ \mu m^2$ (corresponding to the magnification of the real-time observation). The density of the 3D islands was determined at a lower magnification (field of view: $46 \times 46\ \mu m^2$).

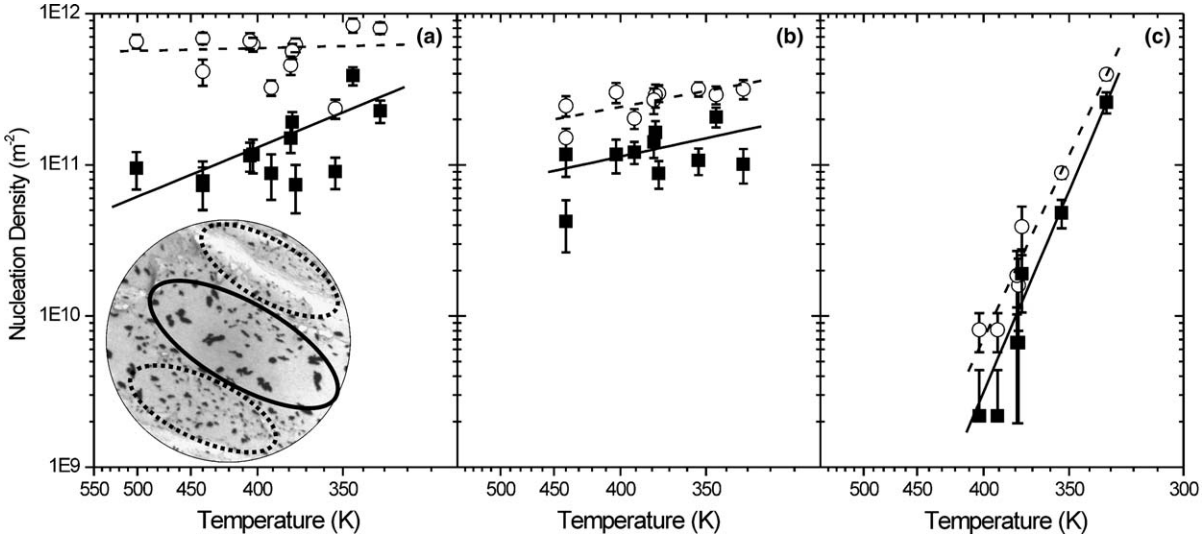

Fig. 3. Arrhenius plots showing the temperature dependence of the nucleation densities of the first (a) and second layer (b), and for 3D islands (c). Different areas on the sample were used for the analysis. The open/full symbols and dashed/solid lines refer to substrate areas with the high/low step density, which are marked in the inset. The parameters for the exponential fit are given in Table 1.

Assuming thermally activated diffusion during nucleation we fitted the following exponential relation to the data (solid or dashed lines for smooth and rough substrate areas, respectively, referring to the different ellipses in the inset of Fig. 3a):

$$n_x(T) = N_0 \exp(E_n/kT), \tag{1}$$

where n_x is the nucleation density at temperature T, k the Boltzmann constant, E_n an activation energy for the nucleation process, and N_0 the exponential prefactor which depends on the deposition rate. The derived fit parameters E_n and N_0 are listed in Table 1.

In general, this temperature dependence is determined by the diffusion and nucleation of the molecules. Unfortunately, up to now no sufficient theoretical description of the growth exists, which involves the specific properties of molecules like, e.g., orientation dependence, non-isotropic bonding to the neighboring molecules, cluster mobility, and internal degrees of freedom. Consequently, atomistic descriptions like those suggested by Venables [16] are oversimplified and can be applied only carefully and in a limited way. Under this simplifying assumption, the energy E_n can be related to the surface diffusion energy E_d and the nucleation energy E_i of a critical cluster of size i

$$E_n = p \cdot (E_d + E_i/i) \tag{2}$$

with $p = i/(i+2)$ and $p = i/(i+2.5)$ for two- and three-dimensional nucleation, respectively. The deposition rate R dependence of the prefactor is given by $N_0 \propto R^p$. The surface diffusion constant is defined as

$$D_{diff} = v \exp\left(-\frac{E_d}{kT}\right) \tag{3}$$

with the attempt frequency v. With the nucleation constant

$$D_{nucl} = v \exp\left(-\frac{E_i}{i \cdot kT}\right) \tag{4}$$

an effective diffusion constant can be defined as $D_{eff} = D_{diff} \cdot D_{nucl}$, so that the relation of Eq. (1) can be expressed as:

$$n_x(T) \propto \left(\frac{R}{D_{eff}}\right)^p. \tag{5}$$

In the following we define the so called "diffusion length" as $L = 1/\sqrt{n_x(T)}$.

The temperature dependence of the nucleation density of the first layer significantly differs for the growth on smooth and on rough substrate areas (Fig. 3a). On the smooth area the nucleation density has an exponential dependence indicating that thermally activated diffusion processes are involved in the nucleation process and in the subsequent growth. In contrast, the 2D island density on the rough substrate area is nearly constant over the whole temperature range of 330–500 K, i.e., no thermally activated process determines the nucleation density. Thus we can conclude that the diffusion length is limited to small areas between step bunches and is hence temperature independent. As consequence, the nucleation and therefore the growth are determined by the substrate morphology, which itself depends on the sample preparation.

The extrapolation of the two fit curves in Fig. 3a (for flat and rough substrate areas) towards lower temperature yields a crossing point at about 300 K. Below this temperature the thermally activated nucleation density is higher than the density of substrate defects or traps (i.e., the diffusion length is smaller than the distance of traps like steps or step bunches) and therefore the growth will not be dominated by substrate morphology effects.

For the second layer the nucleation density of both, the smooth and the rough area depends on the temperature (Fig. 3b). The slope of the fit curves results in activation energies of diffusion of 70 (±30) meV and 58 (±18) meV for the smooth and for the rough area, respectively, which are identical within the error bars (see Table 1). Only the absolute value of the nucleation density is about half an order of magnitude higher for the rough area. Comparing the experimental data of the second and the first layer, the 2D island density on the rough area is significantly smaller for the second than for the first layer. Thus, expectedly the influence of the substrate morphology on the nucleation is reduced if one monolayer of PTCDA covers the substrate.

The 3D island density varies over about *two orders of magnitude* in the small explored temperature range of 80 K. However, the temperature dependence of the 3D island nucleation density (Fig. 3c) differs only weakly for the two different types of surface areas. The substrate morphology also has no influence on the nucleation density, especially at low temperatures. The slope of the fit curves corresponds to an activation energy of about 0.7 eV, which corresponds well to the result of Krause et al. deduced from X-ray diffraction [13]. The activation energy is about one order of magnitude larger than for the first and second layer (Table 1). In contrast, for the 3D islands the pre-factor N_0 is about 9 orders of magnitude smaller than for the first and second layer. This indicates that the nucleus formation of the first and second layer differs from that of the 3D islands. This behavior of a high activation energy and a low pre-factor value was seen for the Stranski–Krastanov growth of metal on metals [16] and of metal on

Table 1
Fit parameters N_0 and E_n for the curves of Fig. 3 describing the temperature T dependence of the island density $n_x = N_0 \exp(E_n/kT)$

Substrate area	1st layer		2nd layer		3D islands	
	Rough	Smooth	Rough	Smooth	Rough	Smooth
N_0 (m^{-2})	$10^{(12\pm1.3)}$	$10^{(9.5\pm0.3)}$	$10^{(10.7\pm0.2)}$	$10^{(10.2\pm0.5)}$	$10^{(1.4\pm0.5)}$	$10^{(0.2\pm1.5)}$
E_n (meV)	10 ± 10	130 ± 20	58 ± 18	70 ± 30	670 ± 40	740 ± 100

Si(1 1 1) [17], which can be explained by a high value of i for the critical cluster size [16], or by the mobility of smaller clusters [17].

4. Discussion

A model describing the influence of step bunches on the nucleation of 2D and 3D islands is depicted in Fig. 4. On smooth surface areas (Fig. 4a) the lateral corrugation of the potential is equal to the activation energy of diffusion E_d. The substrate morphology at step bunches may cause either an attracting (Fig. 4b) or a repelling (Fig. 4c) potential for the diffusing PTCDA molecules. In the first case, the attractive potential offers nucleation sites of constant concentration. As long as the thermally activated diffusion length is larger than the distance between these pinning centers, the nucleation occurs only at defects and is therefore temperature independent.

The second possible case of a repelling potential at step bunches could be due to an Ehrlich–Schwoebel-barrier [18] for the PTCDA molecules at steps. As a consequence the diffusing PTCDA molecules are trapped between these barriers. In each of these trap areas which are surrounded by step bunches the PTCDA molecules diffuse until nucleation occurs. If the diameter of the smooth trap area is considerably smaller than the diffusion length only one nucleus is formed in each trap. Then the overall nucleation density is independent of the temperature and only determined by the density of traps or step bunches.

The situation changes, if a complete monolayer of PTCDA molecules covers the substrate including the step bunches. Now the height of the potential barriers at step bunches is significantly reduced for the molecules diffusing on top of the first layer. By thermal activation it is now easier for the PTCDA molecules to overcome the barrier, resulting in a temperature dependent nucleation density. Consequently, in the case of an attractive potential not every defect (or step bunch) pins molecules or, in the case of repelling barriers, not every trap area is a center of nucleation. Of course, the same is valid for PTCDA molecules diffusing on the second layer and forming 3D islands. The molecules are less disturbed by the step bunches and are able to diffuse over long distances of about 10 μm to create 3D islands (Fig. 2d).

It is interesting to note that single steps which are present also on the smooth areas of the surface have much less influence than step bunches. This can be derived from very recent LEEM experiments on the same system [11] which clearly show single steps also on the smooth areas in between step bunches.

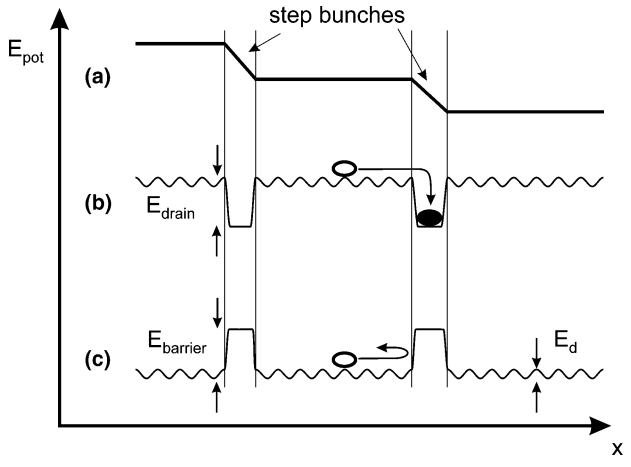

Fig. 4. Model of the potential landscape to illustrate the influence of the step bunches on molecular diffusion. The top scheme (a) depicts a cross sectional view of a surface with two step bunches. The middle (b) and lower (c) drawing show two extreme situations for the potential which a single molecule may sense during diffusion: step bunches acting as drains (b) or barriers (c). The smooth surface has a lateral potential corrugation with the surface diffusion energy E_d. Note that the lateral corrugation of the potential is considerably smaller than the vertical potential which equals the chemical binding energy.

5. Summary and conclusions

The presented PEEM data give first direct experimental evidence of the influence of the substrate morphology on the initial film formation in organic molecular beam epitaxy (OMBE) of PTCDA on Ag(1 1 1). Above room temperature PTCDA films grow in a (slightly modified) Stranski–Krastanov mode. The image sequence during deposition of PTCDA molecules shows a perfect layer-by-layer growth for the first two layers followed by 3D island formation. This behavior reflects the influence of the Ag(1 1 1) metal substrate on the bonding and structural properties, i.e., the strong interaction between substrate and first layer, the weaker interaction between first and second layer causing a strained superstructure of both layers with respect to the (1 0 2) β-PTCDA bulk plane, then a slightly weaker interaction between the following layers leading to the formation of relaxed 3D islands [14].

The diffusion process of PTCDA is strongly influenced by the substrate morphology resulting in a higher nucleation density at rough surface areas. The strongest effect was observed for the nucleation of the first layer, which shows a temperature independent density above room temperature. This behavior can be explained by either attractive or repelling potential barriers at steps. The morphology effects are reduced if one monolayer of PTCDA covers the surface completely.

These results could only be observed by a microscopic probe which can distinguish the inhomogeneous morphology. It demonstrates how difficult an interpretation of integrating measurements (e.g. spectroscopy, diffraction) is which averages the signal over large surface areas. Moreover, the lateral thickness of an organic layer can drastically vary, e.g., by island formation in a Stranski–Krastanov growth mode. Since this may strongly depend on the preparation parameters like surface morphology, temperature, and deposition rate, integral techniques may lead to contradictory results depending on the group, sample, or even on the day of the experiment. We have the

impression that some discrepancies in the literature may be due to such differences.

Acknowledgments

This work was financed by the BMBF under Contracts 05 KS1WW2/0 and 05 KS4WWB/4. One of us (E.U.) likes to thank the Fonds der Chemischen Industrie for support.

References

[1] E. Umbach, R. Fink, in: V.M. Agranovich, G.C. La Rocca (Eds.), Proceedings of the International School of Physics "Enrico Fermi" Course CXLIX, IOS Press, Amsterdam, 2002, p. 233.
[2] F. Schreiber, Phys. Status Solidi A 201 (2004) 1037, and references therein.
[3] G. Witte, C. Wöll, J. Mater. Res. 19 (2004) 1889, and references therein.
[4] M. Schneider, E. Umbach, M. Sokolowski, in this issue, and references therein.
[5] K. Glöckler, C. Seidel, A. Soukopp, M. Sokolowski, E. Umbach, M. Böhringer, R. Berndt, W.D. Schneider, Surf. Sci. 405 (1998) 1.
[6] F. Heringdorf, M.C. Reuter, R.M. Tromp, Nature 412 (2001) 517; F. Heringdorf, M.C. Reuter, R.M. Tromp, Appl. Phys. A 78 (2004) 787.
[7] R. Wichtendahl, R. Fink, H. Kuhlenbeck, D. Preikszas, H. Rose, R. Spehr, P. Hartel, W. Engel, R. Schlögl, H.J. Freund, A.M. Bradshaw, G. Lilienkamp, Th. Schmidt, E. Bauer, G. Benner, E. Umbach, Surf. Rev. Lett. 5 (1998) 1249.
[8] R. Fink, M.R. Weiss, E. Umbach, D. Preikszas, H. Rose, R. Spehr, P. Hartel, W. Engel, R. Degenhardt, R. Wichtendahl, H. Kuhlenbeck, W. Erlebach, K. Ihmann, R. Schlogl, H.J. Freund, A.M. Bradshaw, G. Lilienkamp, Th. Schmidt, E. Bauer, G. Benner, J. Electron Spectrosc. 84 (1997) 231.
[9] Th. Schmidt, U. Groh, R. Fink, E. Umbach, O. Schaff, W. Engel, H.-J. Freund, A.M. Bradshaw, D. Preikszas, P. Hartel, R. Spehr, H. Rose, G. Lilienkamp, E. Bauer, G. Benner, Surf. Rev. Lett. 9 (2002) 223.
[10] Y. Zou, L. Kilian, A. Schöll, Th. Schmidt, R. Fink, E. Umbach, Surf. Sci., in press.
[11] Th. Schmidt, H. Marchetto, U. Groh, R. Fink, H.-J. Freund, E. Umbach, in preparation.
[12] H. Marchetto, U. Groh, Th. Schmidt, R. Fink, H.-J. Freund, E. Umbach, in preparation.
[13] B. Krause, A.C. Dürr, K. Ritley, F. Schreiber, H. Dosch, D. Smilgies, Phys. Rev. B 66 (2002) 235404;
B. Krause, A.C. Dürr, F. Schreiber, H. Dosch, O.H. Seeck, J. Chem. Phys. 119 (2003) 3429;
B. Krause, A.C. Dürr, F. Schreiber, H. Dosch, O.H. Seeck, Surf. Sci. 572 (2004) 385.
[14] L. Kilian, E. Umbach, M. Sokolowski, Surf. Sci. 573 (2004) 359.
[15] L. Chkoda, M. Schneider, V. Shklover, L. Kilian, M. Sokolowski, C. Heske, E. Umbach, Chem. Phys. Lett. 371 (2003) 548.
[16] J.A. Venables, G.D.T. Spiller, M. Hanbucken, Rep. Prog. Phys. 47 (1984) 399.
[17] Th. Schmidt, E. Bauer, Phys. Rev. B 62 (2000) 15815.
[18] G. Ehrlich, F.G. Hudda, J. Chem. Phys. 44 (1966) 1039;
R. Schwoebel, E.J. Shipsey, J. Appl. Phys. 37 (1966) 3682.